Title
Heterogeneous Ozonolysis of Squalene: Gas-Phase Products Depend on Water Vapor Concentration

Authors
Arata, Caleb
Heine, Nadja
Wang, Nijing
et al.

Publication Date
2019-12-06

DOI
10.1021/acs.est.9b05957

Data Availability
The data associated with this publication are in the supplemental files.

Heterogeneous Ozonolysis of Squalene: Gas-Phase Products Depend on Water Vapor Concentration

Caleb Arata*†§, Nadja Heine‡, Nijing Wang¶, Pawel K. Misztal§#, Pawel Wargocki^, Gabriel Bekö^, Jonathan Williams¶, William W Nazaroff‖, Kevin R. Wilson‡, Allen H. Goldstein§‖

†Department of Chemistry, §Department of Environmental Science, Policy and Management, and ‖Department of Civil and Environmental Engineering, University of California, Berkeley, California 94720 United States

‡Chemical Sciences Division, Lawrence Berkeley National Laboratory, Berkeley, California 94720, United States

¶Air Chemistry Department, Max Planck Institute for Chemistry, 55128 Mainz, Germany

^Department of Civil Engineering, Technical University of Denmark, 2800 Kgs. Lyngby, Denmark

Now at: Department of Civil, Architectural and Environmental Engineering, The University of Texas at Austin, Austin, TX 78712

*Phone: 310 968 8331. Email: caleb.arata@berkeley.edu

Abstract

Previous work examining the condensed-phase products of squalene particle ozonolysis found that an increase in water vapor concentration led to lower concentrations of secondary ozonides,

increased concentrations of carbonyls, and smaller particle diameter, suggesting that water changes the fate of the Criegee intermediate. To determine if this volume loss corresponds to an increase in gas-phase products, we measured gas-phase volatile organic compound (VOC) concentrations via proton-transfer-reaction time-of-flight mass spectrometry. Studies were conducted in a flow-tube reactor at atmospherically relevant ozone (O_3) exposure levels (5-30 ppb h) with pure squalene particles. An increase in water vapor concentration led to strong enhancement of gas-phase oxidation products at all tested O_3 exposures. An increase in water vapor from near zero to 70% relative humidity (RH) at high O_3 exposure increased the total mass concentration of gas-phase VOCs by a factor of three. The observed fraction of carbon in the gas-phase correlates with the fraction of particle volume lost. Experiments involving O_3 oxidation of shirts soiled with skin oil confirms that the RH dependence of gas-phase reaction product generation occurs similarly on surfaces containing skin oil under realistic conditions. Similar behavior is expected for O_3 reactions with other surface-bound organics containing unsaturated carbon bonds.

Introduction

People spend 90% of their lives indoors[1]. Each day, adult humans inhale 12-15 kg of air, making indoor air an important route of exposure to many chemicals, including volatile organic

compounds (VOCs). People can be the dominant indoor VOC emission source in densely occupied spaces, and, in the presence of ozone (O_3), the oxidation of skin lipids adds ketones and aldehydes to the composition of indoor air[2–8].

Indoor O_3 concentrations are commonly 20-70% of outdoor levels, with the ratio depending on building air-change rate (ACR), type of ventilation system, and the nature of indoor surfaces[9]. Indoor air is estimated to contribute 25-60% of an individual's daily O_3 exposure.[10] In densely occupied spaces, occupants may be the dominant indoor sinks for O_3, mainly due to reactions with lipids on their skin, hair, and clothing.[11]

Squalene ($C_{30}H_{50}$) constitutes 10% of the mass of human skin lipids, and contributes 50% of the unsaturated carbon bonds.[12] When exposed to O_3, squalene is quickly oxidized to products that span a wide range of volatility; some products remain in the condensed phase while others become gaseous.[5]

Researchers have investigated effects of human occupancy on aircraft cabin air, considering that interior O_3 levels are sometimes elevated in airplanes.[13] Weschler et al. conducted experiments in a simulated aircraft cabin section and found that more than half of the observed oxidation products in the gas phase came from O_3 reacting with human skin lipids.[4] Further work studied O_3 deposition on materials common to aircraft cabin interiors, finding that soiled clothing exposed to O_3 emits 6-methyl-5-hepten-2-one (6-MHO).[14,15] Surface bound

55 squalene was found to have a high reaction probability with O_3, in the range of 0.5-1 × 10^{-3}, and
56 reaction of ozone with squalene on soiled clothing has been shown to be mass-transport
57 limited.[16–18] Both 4-oxopentanal (4-OPA) and 6-MHO are known respiratory irritants.[19,20]
58 Acetone and 6-MHO are among the most prominent VOCs emitted from human skin.[21] While
59 acetone is known to originate from a wide variety of sources, including breath, 6-MHO is
60 thought to be specific to squalene oxidation. The high emission rate suggests that squalene
61 oxidation contributes significantly to VOC emissions from human skin.
62 Heine et al. investigated the influence of RH on squalene ozonolysis using pure squalene
63 particles in a flow-tube reactor.[22] They showed that water vapor concentration does not affect the
64 rate of squalene ozonolysis, but does substantially change the product composition. Under dry
65 conditions, as O_3 consumes squalene, secondary ozonide concentrations increase in the
66 condensed phase and initial particle volume is reduced by 15%. At 60% RH, condensed-phase
67 ozonolysis products shift from secondary ozonides to carbonyls, and particle volume is reduced
68 by as much as 50%. Such losses of particle volume should correspond to an increase in gas-
69 phase oxidation products.
70 For this study, we designed experiments specifically to observe the mass lost to the gas
71 phase and the products formed by O_3-squalene reactions as a function of RH, and to understand
72 the implications for the fate of the Criegee intermediate on squalene particle surfaces and skin-oil

coated clothing. Here, we investigate the gas-phase products from squalene particle ozonolysis in a flow tube reactor, and on skin-oil soiled shirts in a climate chamber. From the flow-tube experiments, we show that the RH dependent loss of particle diameter corresponds to an increase in gas-phase reaction products, consistent with the mechanism of water molecules promoting carbonyl formation from the Criegee intermediate under real world conditions. We discuss implications for product yields from skin oil ozonolysis indoors under varying RH conditions.

Experimental Methods

Squalene ozonolysis was carried out in a flow-tube reactor, as described in Heine et al.[22,23] Liquid squalene in a tube furnace was heated to 145 ºC, generating, by means of homogeneous nucleation, polydisperse particles with a mean surface-weighted diameter of 250 +/- 40 nm. A continuous flow of 300 standard cm^3 min^{-1} dry nitrogen (N_2) carried the particles from the furnace through a charcoal denuder to remove any gas-phase contamination. This flow was then combined with flows of oxygen (O_2), O_3, dry N_2, and humidified N_2 for a total flow of 1 L min^{-1}. Levels of O_2 were held at a constant 10%, while the flows of dry and humidified N_2 were varied to give a range of nearly 0% (< 3%) to 100% RH. This combined flow traversed the flow tube reactor (130 cm long, 2.5 cm inner diameter) with a residence time of 37 s.[24] Ozone was produced by a corona discharge generator, and the concentrations of O_3 were in the range 0-4

ppm, giving O_3 exposures of 0-44 ppb h. The initial particle loading in the flow reactor was 1000 μg m^{-3}.

Upon leaving the flow-tube reactor, the outflow composition was measured by proton-transfer-reaction time-of-flight mass spectrometry (Ionicon PTR-TOF-MS 8000), an electrostatic classifier (TSI model 3080L) with a butanol-based condensation particle counter (TSI model 3772), and a custom-built vacuum ultraviolet aerosol mass spectrometer (VUV-AMS). The particle size and composition measurements are described in Heine et al.[22]; the PTR-TOF-MS was used to measure speciated gas-phase VOC concentrations.

PTR-TOF-MS is a chemical ionization technique with minimal fragmentation using H_3O^+ as the primary reagent ion. PTR-TOF-MS has been previously used to detect gas-phase products of squalene ozonolysis.[2,4,5] For these experiments, the instrument was calibrated with a multicomponent VOC gas standard to ensure stability throughout the campaign. Of the compounds reported here, only acetone was determined using a direct calibration. All other compound concentrations were calculated using a default proton transfer reaction rate constant of 2.5×10^{-9} cm^3 s^{-1} for both the primary ion, H_3O^+, as well as for the first water cluster, $H_3O^+(H_2O)$. Direct calibration accuracies are estimated to be +/- 10%, whereas concentration accuracies derived from the default rate constant are typically +/- 50%.[25] Increases in RH can

cause increases in instrument sensitivities for certain compounds. However, these changes are typically a few percent, much lower than concentration differences reported in this work.[26,27]

Measurements of VOCs at each specified RH and O_3 exposure were made by allowing concentrations in the reactor to stabilize. Once stable, the particle flow was quickly replaced with a flow of N_2. After 2 min, 95% of the particles were removed from the reactor, and a background concentration was taken. To account for both compounds being desorbed from the flow-tube walls as well as compounds being produced by heterogeneous oxidation on the walls, O_3 flow was maintained during the background sampling procedure. The difference between the stable concentration and the background concentration was taken to be the gas-phase concentration attributable to squalene-particle ozonolysis. Tables S1–S5 show the concentrations for each species as measured from the flow tube, as well as the measured background.

An experiment to analyze emissions from skin-oil soiled clothing under varying conditions of RH and O_3 was performed as part of the Indoor Chemical Human Emissions and Reactivity (ICHEAR) project. Four identical T-shirts (100% cotton) were washed with fragrance-free detergent and tumble dried, before being worn by four people overnight (minimum of 8 h). The skin-oil soiled T-shirts were then placed inside a stainless-steel climate chamber (volume 26.8 m^3) ventilated with an air-change rate of 3.2 h^{-1}. Outdoor air was used for ventilation. It was filtered using particle and activated carbon filters to avoid interference from

125 outdoor VOCs, and conditioned to reach the required temperature and RH. Ozone was generated
126 (Jelight Model 600 UV) in the HVAC system downstream of the activated carbon filter and
127 continuously introduced into the chamber at levels between 95-100 ppb. The temperature inside
128 the chamber was maintained at 27.4–28.3 °C during the experiment and the O_3 levels were
129 monitored throughout. Four RH levels were established. The lowest RH levels (at the beginning
130 and end of the experiment) were not controlled (humidifier off, no dehumidifying present), while
131 the two higher RH levels were achieved by operating a steam humidifier in the HVAC system.
132 The first three levels were maintained for 1.5-2 hours to allow steady-state conditions to be
133 reached. The resulting average RH levels during these three periods were 26%, 41%, and 56%.
134 The final, fourth, RH condition was a decay from 50% to 28% with the humidifier off. The
135 average RH for this period was 33%.
136 A PTR-TOF-MS (8000, Ionicon Analytik GmbH Innsbruck, Austria) was deployed
137 during ICHEAR to monitor VOCs produced from O_3 oxidation of skin oil. The operational
138 conditions of the PTR-TOF-MS were drift tube pressure 2.2 mbar, temperature 60 °C and 137 Td
139 (*E*/*N*). The 3.2-mm (1/8") Teflon inlet of the instrument was attached to the main exhaust duct of
140 the chamber, approximately 1 m from the terminal through which the air was exhausted from the
141 chamber and set to draw 100 mL min^{-1} (via a main high flow inlet of 7 L min^{-1}) continuously
142 into the mass spectrometer. Data reported for the skin-oil T-shirt experiment represent sample

time resolution of 20 s. Before putting T-shirts inside the chamber, a background level of the empty chamber was established and maintained for 10 minutes. The measured background VOC levels were subsequently subtracted from the VOC levels measured while the T-shirts were in the chamber.

Results and Discussion

Figure 1 shows the chemical structures of squalene and selected gas-phase ozonolysis products. The first-generation gas-phase products are acetone, 6-methyl-5-hepten-2-one (6-MHO), and geranylacetone. Terminal oxidation products found in the gas phase, i.e. products that are minimally reactive with O_3 because of their lack of carbon-carbon double bonds, are acetone, 4-oxopentanal (4-OPA), and 1,4-butanedial (succinaldehyde). Scheme 1 shows a simplified mechanism for alkenes reacting with O_3. In **R1**, O_3 adds across the double bond, forming a primary ozonide (not shown), which quickly decomposes to one of two combinations of carbonyl and Criegee intermediate. This reaction is fast and does not include water, so water vapor concentration has no effect on the rate of alkene loss.[22] The Criegee intermediate produced by **R1** is reactive, and can proceed through **R2** or **R3**, as well as through rearrangement or reactions with carboxylic acids[28,29]. **R2** shows the Criegee intermediate reacting with water to form the α-hydroxyhydroperoxide, which decomposes to a carbonyl and to hydrogen peroxide.

160 **R3** shows the Criegee intermediate reacting with another carbonyl to form a secondary ozonide.
161 The carbonyl products are more volatile than their respective secondary ozonides; in the
162 presence of water, **R2** occurs faster than **R3**, leading to greater release of reaction products to the
163 gas phase and a concomitant shrinking of the particle.

164 Figures 2A and 2B show the gas-phase concentration of geranylacetone and 6-MHO
165 exiting the flow-tube reactor as a function of O_3 exposure and RH. Both compounds are primary
166 products of squalene oxidation, and both have carbon-carbon double bonds that can further react
167 with O_3. At all RH levels, geranylacetone production peaks at an O_3 exposure of 10 ppb h. Dry
168 conditions yield 5 μg m^{-3} of geranylacetone, whereas more humid conditions (70% RH) enhance
169 the concentration to 19 μg m^{-3}, an increase by almost 4×. More humid conditions, specifically
170 RH of 30% and 50%, also show an increase in geranylacetone concentration compared to dry
171 conditions. At exposures of 20 ppb h, the geranylacetone is fully consumed by ozonolysis and is
172 not detected. Compared to other products measured, concentrations of geranylacetone are small.
173 As a 13-carbon ketone, with a vapor pressure of 3.5 Pa at 298 K, most of the geranylacetone is
174 expected to remain in the condensed phase.[6] Furthermore, there are fewer possible reaction
175 pathways to produce geranylacetone than the other, shorter chain products. The low
176 concentration measured in this study is consistent with a classroom study by Tang et al., where
177 both 6-MHO and 4-OPA were found at significantly higher concentrations than geranylacetone.[2]

178 The production of 6-MHO shows strong RH dependence. At all levels of O_3 exposure, an
179 increase in RH leads to an increase in 6-MHO concentration. As 6-MHO is a primary product
180 that can also be consumed, peak concentrations are found at the lower levels of O_3 exposure. At
181 70% RH and 12 ppb h of O_3 exposure, the detected concentration is 170 μg m^{-3}, 3 times the level
182 of 6-MHO detected at the same O_3 exposure but under dry conditions. Unlike geranylacetone, 6-
183 MHO is detected at even the highest levels of O_3 exposure tested, 30 ppb h. The 6-MHO species
184 is used as a primary tracer compound for squalene oxidation, along with 4-OPA as a secondary
185 tracer. The fact that 6-MHO is consumed at higher O_3 exposures, while 4-OPA is not, suggests
186 that 6-MHO concentrations could be used as a proxy indicator for the age of oxidation products:
187 at longer timescales, 6-MHO becomes depleted while 4-OPA does not.
188 Figures 3A-3C show the gas-phase concentrations as a function of O_3 exposure and RH
189 of the three terminal products: acetone, 4-OPA, and 1,4-butanedial. At most levels of O_3
190 exposure, increasing RH produces increasing concentrations of acetone, again showing strong
191 humidity dependence. At very low O_3 exposure (5-6 ppb h), 30% RH produces 32 μg m^{-3} of
192 acetone, whereas 70% RH conditions give 77 μg m^{-3}, an increase by more than 2×. Under dry
193 conditions, acetone increases to 100 μg m^{-3} at 12 ppb h exposure, and then does not increase with
194 increasing O_3 exposure. As acetone does not have carbon-carbon double bonds, it does not react
195 significantly with O_3 and so increasing exposure is not expected to consume acetone. Under

196 higher RH conditions, the same leveling off is seen, but at higher concentrations. At 70% RH,
197 acetone concentrations begin to plateau at 20 ppb h exposure, at a concentration of 280 μg m^{-3}.
198 At O_3 exposures greater than 10 ppb h, increasing RH from 0% to 70% increases acetone
199 concentrations by a factor of 2.5 to 3.
200 Figure 3B shows the RH dependence of 4-OPA from the ozonolysis of squalene. A
201 minimum of two reactions involving O_3 are required to produce 4-OPA from squalene, so
202 concentrations are observed to increase later than the primary products, acetone and 6-MHO.
203 Despite being a terminal product, 4-OPA does not show the same leveling off behavior as
204 acetone. Under dry conditions, production stops increasing at 20 ppb h O_3 exposure, but under
205 high RH conditions no leveling off is seen; production of 4-OPA may increase past 30 ppb h
206 exposure. At O_3 exposures less than 12 ppb h, no RH dependence is seen, but production is also
207 small. At higher O_3 exposures, 4-OPA shows strong RH dependence, with a factor of 6 increase
208 in concentration between dry and humid conditions at 30 ppb h O_3 exposure. In both mixing ratio
209 and mass concentration, 4-OPA is the most abundant gas-phase product, with a peak
210 concentration of 600 μg m^{-3}. If each double bond in squalene proceeds through reaction **R2**, one
211 molecule of squalene would produce a single 1,4-butanedial molecule, two acetone molecules,
212 and four 4-OPA molecules. While the observed mixing ratios of terminal products do not follow
213 these stoichiometric ratios, the relatively large number of 4-OPA molecules that can be made

214 from each squalene molecule help to explain why it is the most abundant gas-phase product.

215 Figure 3C shows the concentration of 1,4-butanedial as a function of RH and O_3

216 exposure. As a terminal product, abundance of this species increases with O_3 exposure, and, for

217 some RH conditions, eventually levels off. As with 4-OPA, production of 1,4-butanedial requires

218 a minimum of two ozonolysis reactions, so concentrations substantially increase at greater O_3

219 exposure. Production of 1,4-butanedial shows a more complicated relation to RH than other

220 species. The lowest levels of production, across all O_3 exposures, are under the most humid

221 conditions. The next lowest levels of production are under the driest conditions. Although it does

222 not follow the pattern of the other species measured, 1,4-butanedial levels do show strong

223 variability with RH. At 30 ppb h O_3 exposure, switching from 70% RH to 30% RH increases the

224 concentration of 1,4-butanedial from 52 μg m^{-3} to 140 μg m^{-3}. This ~3× increase in production is

225 in line with the 3-6× changes in production observed at different RH for other compounds. The

226 fact that 1,4-butanedial production peaks at intermediate RH, and declines at low and high RH,

227 suggests that water plays a more complicated role than depicted in Scheme 1. Specifically,

228 reaction **R2** increases 1,4-butanedial production up to a point, and then facilitates other reactions

229 that suppress production.

230 Wisthaler and Weschler (2010) observed 12 prominent VOCs from squalene ozonolysis,

231 including the five compounds already discussed.[5] When glass wool soiled with human skin oil

232 was exposed to O_3 (0-75 ppb h), three species — 4-methyl-8-oxo-4-nonenal (4-MON), 4-methyl-
233 4-octene-1,8-dial (4-MOD), and 1-hydroxy-6-methyl-5-hepten-2-one (OH-6MHO) — showed
234 mixing ratios similar to the observed mixing ratios of 4-OPA and 1,4-butanedial. These species
235 were also observed during ozonolysis of a pure squalene film; however, the mixing ratios for that
236 experiment were not reported. In our work, all three compounds were detected (4-MON, 4-
237 MOD, and OH-6MHO), but at very low concentrations, 2 μg m^{-3} or less. Possibly due to the low
238 concentration of these species, a RH dependence isn't discernible.
239 Four other compounds identified by Wisthaler and Weschler (2010) — 1-hydroxypropan-
240 2-one (hydroxyacetone), 4-oxobutanoic acid, and the isobaric compounds 5-hydroxy-4-
241 oxopentanal and 4-oxopentanoic acid (levulinic acid) — are found in the present work at peak
242 concentrations much lower than 6-MHO, acetone, 4-OPA, and 1,4-butanedial (5-15 μg m^{-3}
243 versus 140-600 μg m^{-3}). All four compounds are terminal products; concentrations either
244 increase or level off with increasing O_3 exposure, and none of the products show increasing
245 production with increasing RH. Hydroxyacetone shows a muted response to changes in RH, as
246 seen in Figure S1. Production is similar at 30% RH, 50% RH, and 70% RH, but increase by ~50-
247 100% under dry conditions. Concentrations are modest, peaking at 15 μg m^{-3} under dry
248 conditions and 30 ppb h O_3 exposure. Levulinic acid or 5-hydroxy-4-oxopentanal (or a
249 combination of the two) only shows a RH effect at the highest O_3 exposure. At 30 ppb h, 70%

RH yields 7 μg m^{-3} while 30% RH produces 15 μg m^{-3}, as seen in Figure S2. Figure S3 shows 4-oxobutanoic acid production *decreasing* with increased RH. At 70% RH and 30 ppb h O_3 exposure, we observe 1 μg m^{-3}, whereas under dry conditions we measure 5 μg m^{-3}.

One fragmentation ion was produced in quantities comparable to those of the dominant products, *m/z* 43.018 Da, $C_2H_3O^+$. This fragment is common to acetic acid and acetate esters, but ions consistent with these parent masses were only found in low concentrations, so it is unassigned.[30] The fragment was found at mixing ratios comparable to 1,4-butanedial, and shows similar responses to RH.

To explore whether our gas-phase measurements agree with the amount of material lost from the particle phase, we summed the amount of carbon detected in the gas-phase products at different levels of RH. We used a carbon-balance approach to test whether the loss of material from the particle phase could be accounted for by generation of gas-phase products. The concentration of squalene entering the flow tube reactor was 1000 μg m^{-3}, corresponding to 880 μg m^{-3} of carbon. Converting the measurements in Figures 2-3 from μg m^{-3} to μg C m^{-3}, and normalizing to the initial concentration of carbon entering the flow tube, gives the percent carbon in the gas phase. (As with the reported concentrations, these measurements are accurate to +/- 50% for all species except for acetone, which is accurate to +/- 10% because it is directly calibrated.) Figure 4 shows the percent carbon in the gas phase at 20 ppb h O_3 exposure. Note

268 that only the dominant products are shown. Switching from 0% RH to 70% RH increases the
269 proportion of carbon entering the gas phase from 21% to 65%, with increases in all dominant
270 products except 1,4-butanedial. Assuming that an average of two molecules of oxidation
271 products are generated for each molecule of ozone that reacts with squalene, this outcome
272 corresponds to yields of between 42% and 130% for gas-phase oxidation products per molecule
273 of ozone consumed. Even a moderate change, from dry conditions to 30% RH, increases the
274 proportion of carbon entering the gas phase by 60%. The largest increases are seen in 4-OPA
275 production.

276 Because the VUV-AMS only measures relative concentrations of species, there is no
277 direct measurement of the amount of carbon present in the condensed phase. However,
278 measurements of the change in particle volume can be used as a quantitative indicator for mass
279 loss from the particle. Note that this approach ignores any mass gained by the addition of oxygen
280 to condensed phase products of ozonolysis, as well as any difference in densities between
281 squalene and condensed-phase reaction products. Despite these limitations, using this approach,
282 there is a clear and strong correlation between the carbon detected in the gas phase and the
283 volume lost from the particle, as shown in Figure 5. Under dry conditions, at all levels of O_3
284 exposure, ~20% of the particle volume is lost, and ~20% of the carbon from squalene is found in
285 the gas phase. At higher RH values, both the particle volume lost and the amount of carbon

286 entering the gas phase are more sensitive to O_3 exposure, as shown by the larger spread for these
287 humidified conditions. The highest RH level (70%) gives both the greatest particle volume loss
288 and the largest percent of carbon in the gas phase. Notwithstanding experimental uncertainties,
289 the evidence displayed in Figure 5 is consistent with expectations for the quantitative loss of
290 particle-phase carbon being balanced with increased abundances of gaseous carbon species.
291 Figures 6 and S4 show the measurements in chamber air of several pertinent VOCs along
292 with O_3 and RH. Four T-shirts were placed inside the measurement chamber at 10:25 with RH
293 maintained at ~26% for 1.5 h. Thereafter the RH was increased in a series of steps. The
294 previously identified squalene oxidation products (4-OPA, 1,4-butanedial, acetone, 6-MHO, and
295 geranylacetone) were observed to vary in response to the changing RH levels. Owing to the
296 working principle of the humidifier, the RH in the chamber fluctuated regularly within a 10%
297 range with a cycle of 38 minutes. In the data shown, primary unsaturated products and terminal
298 products all faithfully follow the RH variation, confirming the dependence of gas-phase squalene
299 ozonolysis products on RH, consistent with the flow-tube experiments. In accordance with
300 previous studies, 4-OPA was the most abundant product (especially at higher RH levels);
301 geranylacetone concentration was consistently the lowest among the quantified species.
302 In contrast with the flow-tube experiment, in which squalene particles were continuously
303 supplied, the skin-oil soiled T-shirts contained a limited amount of squalene that was

304 progressively consumed by O_3. Therefore, at any given RH, most of the compounds showed a
305 decreasing trend as the available squalene was depleted, except the first level where the lagging
306 terminal products still increase towards steady state. In particular, acetone clearly followed the
307 RH modulation while steadily decreasing as the experiment progressed. To better quantify the
308 relative yields of the VOCs as a function of RH, two pairs of RH levels were selected,
309 corresponding to points labeled 1-4 in Figure 6. As shown in Table 1, the concentration of 4-
310 OPA increased by 5.9 μg m^{-3} as the RH increased from 26% (point 1) to 44% (point 2). A
311 similar increase of 5.1 μg m^{-3} was seen in a second cycle as the RH changed from 46% (point 3)
312 to 59% (point 4). The other terminal products (1,4-butanedial, hydroxy acetone, 4-oxobutanoic
313 acid and 5-hydroxy-4-oxopentanal/levulinic acid) also showed slightly higher yields during the
314 first RH increase (point 1 to point 2). Although the level of the first-generation products
315 (acetone, 6-MHO and geranylacetone) tended to decrease with time, an increase was still
316 observed in the second step (points 3 and 4) when the RH increased from 46% to 59%. However,
317 unlike 4-OPA, the concentration changes were much lower than during the first RH increase
318 (points 1 and 2), as shown in Table 1. For 6-MHO and geranylacetone, additional oxidation by
319 O_3 could also be a contributing factor. Ozone removal was 3.4 ppb in the second RH step (46%
320 to 59%), compared to 2.9 ppb in the first step, indicating that more 6-MHO and geranylacetone
321 were produced and subsequently oxidized by O_3 at this stage. Significantly elevated 4-OPA

322 concentrations after the second increase of RH further supports this explanation.

323 Effects of RH on squalene ozonolysis have been observed in prior studies. Petrick and
324 Dubowski studied the condensed phase of squalene film oxidation while varying RH, finding
325 that increased RH led to more ketone production.[31] They also note that RH did not influence
326 reaction kinetics, a finding also reported by Fu et al.[32] Wang and Waring examined secondary
327 organic aerosol formation from the ozonolysis of surface-film squalene at 21% RH and 51%
328 RH.[33] At high O_3 exposures, they found that the higher RH increased the aerosol mass fraction
329 (AMF) from squalene. This increase suggests that higher RH leads to more oxidation products
330 entering the gas phase, where they then can condense onto airborne particles. Zhou et al.
331 examined the RH dependence of squalene film oxidation on the condensed phase products,
332 finding that increasing the RH increased the yield of lower molecular weight products and
333 decreased the yield of higher molecular weight products.[34] Although not quantitatively
334 comparable, these previous studies qualitatively agree that an increase in RH leads to an increase
335 in volatile products from squalene ozonolysis.

336 Humidity is already known to be an important factor that can influence VOC emissions
337 from materials, compete with VOCs for sorptive uptake, and influence how indoor air is
338 perceived.[35–44] Humidity is also known to change the rate of uptake of O_3 on indoor surfaces, a
339 relationship that varies among common indoor materials.[45] Few studies have assessed how RH

340 changes ozonolysis products and emission rates. Coleman et al. (2008) found that increasing RH
341 from 10% to 50% doubled the emissions of most ozonolysis byproducts from a cotton surface,
342 with nonanal and decanal emissions increasing by about 5×.[14] Gall et al. (2013) studied primary
343 and secondary ozonolysis emissions from building materials, finding RH to have mixed effects.[46]
344 Secondary emissions increased with RH for painted drywall, while emissions from carpet and
345 ceiling tile did not. The present work contributes new knowledge, showing that RH can directly
346 influence the products of squalene ozonolysis, providing an alternate route by which water vapor
347 can increase VOC concentrations. At realistic indoor O_3 exposures, a change from 0% RH to
348 70% RH results in ~3 times the amount of carbon entering the gas phase. Squalene, with six
349 carbon-carbon double bonds, is a model molecule to show this effect. Other unsaturated
350 compounds, especially those with double bonds separating small moieties, may show similar
351 behavior. The reactions shown in Scheme 1 are not specific to squalene, and so long as the
352 carbonyls formed by reaction **R2** have sufficient volatility, increased production of gas-phase
353 products are generally expected from increases in RH.

354 The effects seen in this study suggest that RH can significantly alter the gas-phase
355 composition of indoor air. In high occupancy settings, skin-oil oxidation can be the dominant
356 source of VOCs, and changes in RH can alter the strength of this source by as much as a factor
357 of 3.[4] In the flow-tube reactor, at the highest level of O_3 exposure and RH, the sum of the

concentrations of dominant products was 940 μg m^{-3}, comparable to the 1000 μg m^{-3} of squalene entering the reactor. It should be noted that RH does not change the rate of squalene ozonolysis: at low RH, oxidized products are still being formed, but remain in the condensed phase. If that condensed phase is the skin surface, then the products might be taken up dermally, where they might influence health.[19,47] The large effect of RH on ozonolysis products from squalene, and the potential for the underlying mechanism to act on other alkenes, warrants further research on how humidity may modulate indoor reactive chemistry and its consequences.

Supporting Information. Tables of raw and background concentrations of species measured for this study. Figures for species not seen in large quantities.

Acknowledgments. The UC Berkeley team was funded by the Alfred P. Sloan Foundation via Grant 2016-7050. Kevin R. Wilson and Nadja Heine were supported by the Department of Energy, Office of Science, Office of Basic Energy Sciences, Chemical Sciences, Geosciences, and Biosciences Division, in the Gas Phase Chemical Physics Program under Contract No. DE-AC02-05CH11231. This research used resources of the Advanced Light Source, which is a DOE Office of Science User Facility under contract no. DE-AC02-05CH11231. The ICHEAR team (MPI and DTU) were funded by the Alfred P. Sloan Foundation via Grant G-2018-11233. Allen H. Goldstein gratefully acknowledges a Humboldt Research Award from the Alexander von

Humboldt Foundation. The authors gratefully acknowledge members of the ICHEAR team including Nora Zannoni, Mengze Li, and Lisa Ernle for their contributions in performing the T-shirt experiments.

References

(1) Klepeis, N. E.; Nelson, W. C.; Ott, W. R.; Robinson, J. P.; Tsang, A. M.; Switzer, P.; Behar, J. V; Hern, S. C.; Engelmann, W. H. The National Human Activity Pattern Survey (NHAPS): A Resource for Assessing Exposure to Environmental Pollutants. *J. Exposure Anal. Environ. Epidemiol.* **2001**, *11*, 231–252.

(2) Tang, X.; Misztal, P. K.; Nazaroff, W. W.; Goldstein, A. H. Volatile Organic Compound Emissions from Humans Indoors. *Environ. Sci. Technol.* **2016**, *50*, 12686–12694.

(3) Weschler, C. J. Roles of the human occupant in indoor chemistry. *Indoor Air* **2016**, *26*, 6–24.

(4) Weschler, C. J.; Wisthaler, A.; Cowlin, S.; Tamás, G.; Strøm-Tejsen, P.; Hodgson, A. T.; Destaillats, H.; Herrington, J.; Zhang, J.; Nazaroff, W. W. Ozone-Initiated Chemistry in an Occupied Simulated Aircraft Cabin. *Environ. Sci. Technol.* **2007**, *41*, 6177–6184.

(5) Wisthaler, A.; Weschler, C. J. Reactions of ozone with human skin lipids: Sources of carbonyls, dicarbonyls, and hydroxycarbonyls in indoor air. *Proc. Natl. Acad. Sci.* **2010**, *107*, 6568–6575.

(6) Lakey, P. S. J.; Wisthaler, A.; Berkemeier, T.; Mikoviny, T.; Pöschl, U.; Shiraiwa, M. Chemical kinetics of multiphase reactions between ozone and human skin lipids: implications for indoor air quality and health effects. *Indoor Air* **2017**, *27*, 816–828.

(7) Lakey, P. S. J.; Morrison, G. C.; Won, Y.; Parry, K. M.; von Domaros, M.; Tobias, D. J.; Rim, D.; Shiraiwa, M. The impact of clothing on ozone and squalene ozonolysis products in indoor environments. *Commun. Chem.* **2019**, *2*, 56.

(8) Kruza, M.; Carslaw, N. How do breath and skin emissions impact indoor air chemistry? *Indoor Air* **2019**, *29*, 369–379.

(9) Weschler, C. J. Ozone in indoor environments: Concentration and chemistry. *Indoor Air* **2000**, *10*, 269–288.

(10) Weschler, C. J. Ozone's Impact on Public Health: Contributions from Indoor Exposures to Ozone and Products of Ozone-Initiated Chemistry. *Environ. Health Perspect.* **2006**, *114*, 1489–1496.

(11) Fischer, A.; Ljungström, E.; Langer, S. Ozone removal by occupants in a classroom. *Atmos. Environ.* **2013**, *81*, 11–17.

(12) Nicolaides, N. Skin Lipids: Their Biochemical Uniqueness. *Science.* **1974**, *186*, 19–26.

(13) Bhangar, S.; Cowlin, S. C.; Singer, B. C.; Sextro, R. G.; Nazaroff, W. W. Ozone Levels in Passenger Cabins of Commercial Aircraft on North American and Transoceanic Routes. *Environ. Sci. Technol.* **2008**, *42*, 3938–3943.

(14) Coleman, B. K.; Destaillats, H.; Hodgson, A. T.; Nazaroff, W. W. Ozone consumption and volatile byproduct formation from surface reactions with aircraft cabin materials and clothing fabrics. *Atmos. Environ.* **2008**, *42*, 642–654.

(15) Wisthaler, A.; Tamás, G.; Wyon, D. P.; Strøm-Tejsen, P.; Space, D.; Beauchamp, J.; Hansel, A.; Märk, T. D.; Weschler, C. J. Products of Ozone-Initiated Chemistry in a Simulated Aircraft Environment. *Environ. Sci. Technol.* **2005**, *39*, 4823–4832.

(16) Wells, J. R.; Morrison, G. C.; Coleman, B. K. Kinetics and Reaction Products of Ozone and Surface-Bound Squalene. *J. ASTM Int.* **2008**, *5*, 101629.

(17) Jacobs, M. I.; Xu, B.; Kostko, O.; Heine, N.; Ahmed, M.; Wilson, K. R. Probing the Heterogeneous Ozonolysis of Squalene Nanoparticles by Photoemission. *J. Phys. Chem. A* **2016**, *120*, 8645–8656.

(18) Salvador, C. M.; Bekö, G.; Weschler, C. J.; Morrison, G.; Le Breton, M.; Hallquist, M.; Ekberg, L.; Langer, S. Indoor ozone/human chemistry and ventilation strategies. *Indoor Air* **2019**, *29*, 913–925.

(19) Anderson, S. E.; Franko, J.; Jackson, L. G.; Wells, J. R.; Ham, J. E.; Meade, B. J. Irritancy and Allergic Responses Induced by Exposure to the Indoor Air Chemical 4-Oxopentanal. *Toxicol. Sci.* **2012**, *127*, 371–381.

(20) Wolkoff, P.; Larsen, S. T.; Hammer, M.; Kofoed-Sørensen, V.; Clausen, P. A.; Nielsen, G. D. Human reference values for acute airway effects of five common ozone-initiated terpene reaction products in indoor air. *Toxicol. Lett.* **2013**, *216*, 54–64.

(21) Mochalski, P.; King, J.; Unterkofler, K.; Hinterhuber, H.; Amann, A. Emission rates of selected volatile organic compounds from skin of healthy volunteers. *J. Chromatogr. B.* **2014**, *959*, 62–70.

(22) Heine, N.; Houle, F. A.; Wilson, K. R. Connecting the Elementary Reaction Pathways of Criegee Intermediates to the Chemical Erosion of Squalene Interfaces during Ozonolysis. *Environ. Sci. Technol.* **2017**, *51*, 13740–13748.

(23) Heine, N.; Arata, C.; Goldstein, A. H.; Houle, F. A.; Wilson, K. R. Multiphase Mechanism for the Production of Sulfuric Acid from SO2by Criegee Intermediates

Formed during the Heterogeneous Reaction of Ozone with Squalene. *J. Phys. Chem. Lett.* **2018**, *9*, 3504–3510.

(24) Smith, J. D.; Kroll, J. H.; Cappa, C. D.; Che, D. L.; Liu, C. L.; Ahmed, M.; Leone, S. R.; Worsnop, D. R.; Wilson, K. R. The heterogeneous reaction of hydroxyl radicals with sub-micron squalane particles: a model system for understanding the oxidative aging of ambient aerosols. *Atmos. Chem. Phys* **2009**, *9*, 3209–3222.

(25) Zhao, J.; Zhang, R. Proton transfer reaction rate constants between hydronium ion (H_3O^+) and volatile organic compounds. *Atmos. Environ.* **2004**, *38*, 2177–2185.

(26) Kari, E.; Miettinen, P.; Yli-Pirilä, P.; Virtanen, A.; Faiola, C. L. PTR-ToF-MS product ion distributions and humidity-dependence of biogenic volatile organic compounds. *Int. J. Mass Spectrom.* **2018**, *430*, 87–97.

(27) Vlasenko, A.; MacDonald, A. M.; Sjostedt, S. J.; Abbatt, J. P. D. Formaldehyde measurements by proton transfer reaction - mass spectrometry (PTR-MS): correction for humidity effects. *Atmos. Meas. Tech.* **2010**, *3*, 1055–1062.

(28) Zhou, S.; Joudan, S.; Forbes, M. W.; Zhou, Z.; Abbatt, J. P. D. Reaction of Condensed-Phase Criegee Intermediates with Carboxylic Acids and Perfluoroalkyl Carboxylic Acids. *Environ. Sci. Technol. Lett.* **2019**, *6*, 243–250.

(29) Zhao, R.; Kenseth, C. M.; Huang, Y.; Dalleska, N. F.; Kuang, X. M.; Chen, J.; Paulson, S. E.; Seinfeld, J. H. Rapid Aqueous-Phase Hydrolysis of Ester Hydroperoxides Arising from Criegee Intermediates and Organic Acids. *J. Phys. Chem. A* **2018**, *122*, 5190–5201.

(30) Pagonis, D.; Sekimoto, K.; de Gouw, J. A Library of Proton-Transfer Reactions of H_3O^+ Ions Used for Trace Gas Detection. *J. Am. Soc. Mass Spectrom.* **2019**, *30*, 1330–1335.

(31) Petrick, L.; Dubowski, Y. Heterogeneous oxidation of squalene film by ozone under various indoor conditions. *Indoor Air* **2009**, *19*, 381–391.

(32) Fu, D.; Leng, C.; Kelley, J.; Zeng, G.; Zhang, Y.; Liu, Y. ATR-IR Study of Ozone Initiated Heterogeneous Oxidation of Squalene in an Indoor Environment. *Environ. Sci. Technol.* **2013**, *47*, 10611–10618.

(33) Wang, C.; Waring, M. S. Secondary organic aerosol formation initiated from reactions between ozone and surface-sorbed squalene. *Atmos. Environ.* **2014**, *84*, 222–229.

(34) Zhou, S.; Forbes, M. W.; Abbatt, J. P. D. Kinetics and Products from Heterogeneous Oxidation of Squalene with Ozone. *Environ. Sci. Technol.* **2016**, *50*, 11688–11697.

(35) Markowicz, P.; Larsson, L. Influence of relative humidity on VOC concentrations in indoor air. *Environ. Sci. Pollut. Res.* **2015**, *22*, 5772–5779.

(36) Andersen, I.; Lundqvist, G. R.; Mølhave, L. Indoor Air Pollution Due to Chipboard Used as a Construction Material. *Atmos. Environ.* **1975**, *9*, 1121–1127.

(37) Fang, L.; Clausen, G.; Fanger, P. O. Impact of temperature and humidity on chemical and sensory emissions from building materials. *Indoor Air* **1999**, *9*, 193–201.

(38) Huang, H.; Haghighat, F.; Blondeau, P. Volatile organic compound (VOC) adsorption on material: influence of gas phase concentration, relative humidity and VOC type. *Indoor Air* **2006**, *16*, 236–247.

(39) Huang, S.; Xiong, J.; Cai, C.; Xu, W.; Zhang, Y. Influence of humidity on the initial emittable concentration of formaldehyde and hexaldehyde in building materials: experimental observation and correlation. *Sci. Rep.* **2016**, *6*, 23388.

(40) Liang, W.; Yang, S.; Yang, X. Long-Term Formaldehyde Emissions from Medium-

Density Fiberboard in a Full-Scale Experimental Room: Emission Characteristics and the Effects of Temperature and Humidity. *Environ. Sci. Technol.* **2015**, *49*, 10349–10356.

(41) Parthasarathy, S.; Maddalena, R. L.; Russell, M. L.; Apte, M. G. Effect of Temperature and Humidity on Formaldehyde Emissions in Temporary Housing Units. *J. Air Waste Manag. Assoc.* **2011**, *61*, 689–695.

(42) Sidheswaran, M.; Chen, W.; Chang, A.; Miller, R.; Cohn, S.; Sullivan, D.; Fisk, W. J.; Kumagai, K.; Destaillats, H. Formaldehyde Emissions from Ventilation Filters under Different Relative Humidity Conditions. *Environ. Sci. Technol.* **2013**, *47*, 5336–5343.

(43) Xu, J.; Zhang, J. S. An experimental study of relative humidity effect on VOCs' effective diffusion coefficient and partition coefficient in a porous medium. *Build. Environ.* **2011**, *46*, 1785–1796.

(44) Won, D.; Corsi, R. L.; Rynes, M. Sorptive interactions between VOCs and indoor materials. *Indoor Air* **2001**, *11*, 246–256.

(45) Shen, J.; Gao, Z. Ozone removal on building material surface: A literature review. *Build. Environ.* **2018**, *134*, 205–217.

(46) Gall, E.; Darling, E.; Siegel, J. A.; Morrison, G. C.; Corsi, R. L. Evaluation of three common green building materials for ozone removal, and primary and secondary emissions of aldehydes. *Atmos. Environ.* **2013**, *77*, 910–918.

(47) Anderson SE, Franko J, Jackson LG, Wells J, Ham JE, Meade B. Irritancy and allergic responses induced by exposure to the indoor air chemical 4-oxopentanal. *Toxicol Sci.* **2012**, 127, 371–381.

507

508

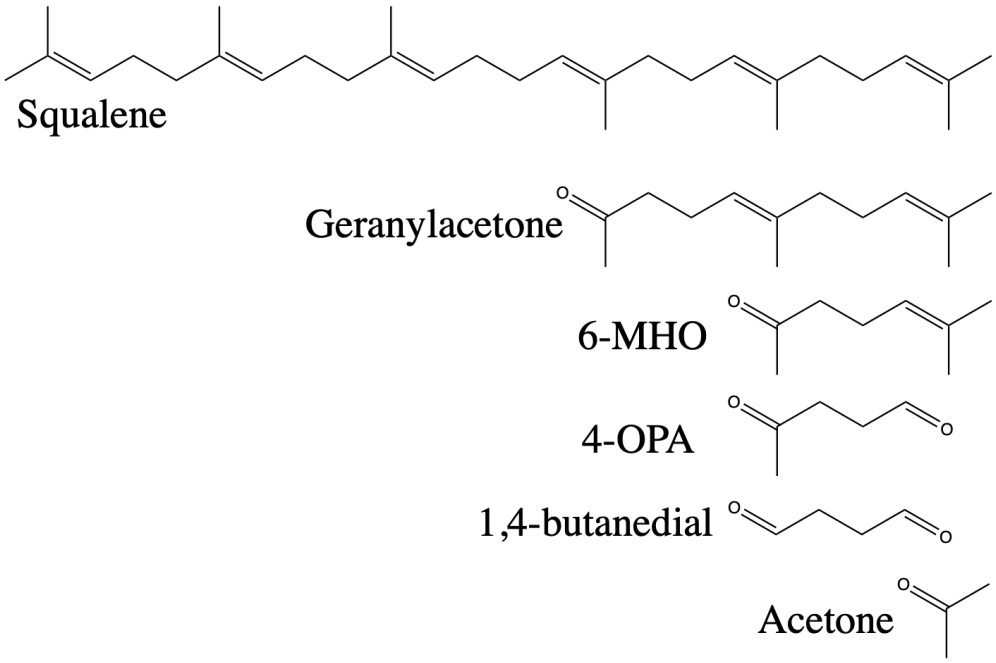

Figure 1: Chemical structure of squalene and selected squalene ozonolysis products

Scheme 1: Simplified Reaction Mechanism for Ozonolysis of Alkenes

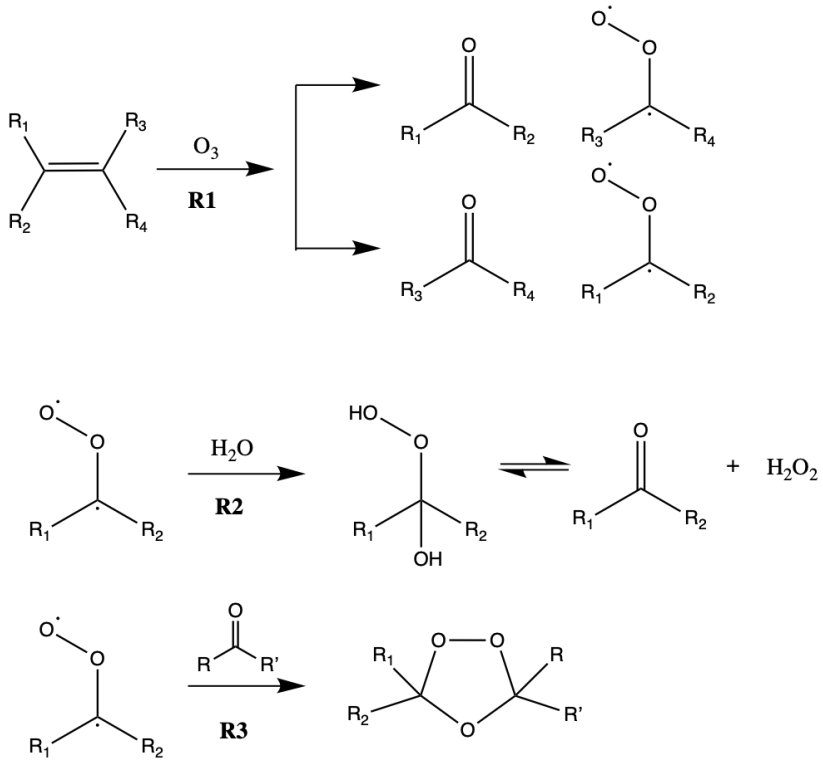

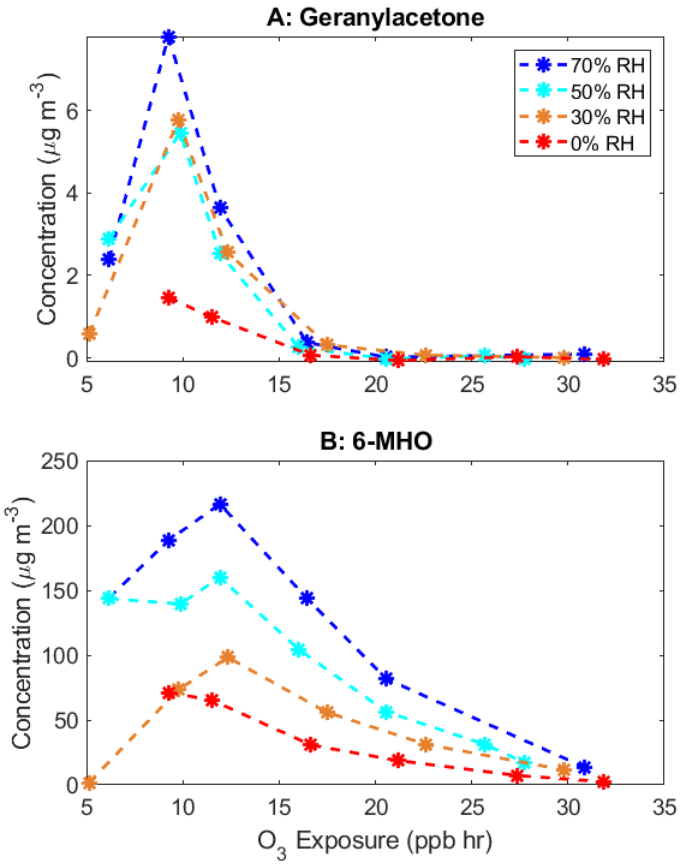

Figure 2: Primary unsaturated products from squalene ozonolysis as a function of humidity and O_3 exposure.

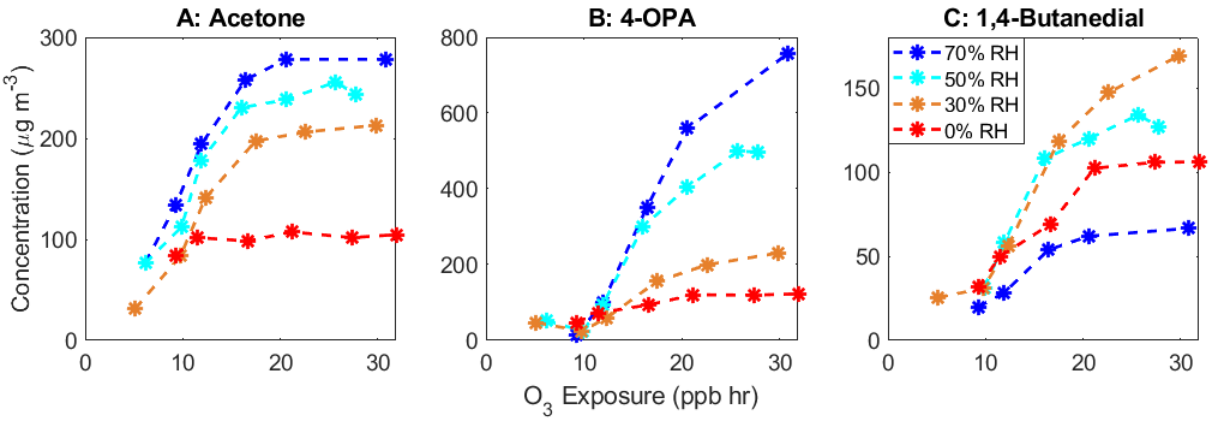

Figure 3: Terminal products from squalene ozonolysis as a function of humidity and O_3 exposure.

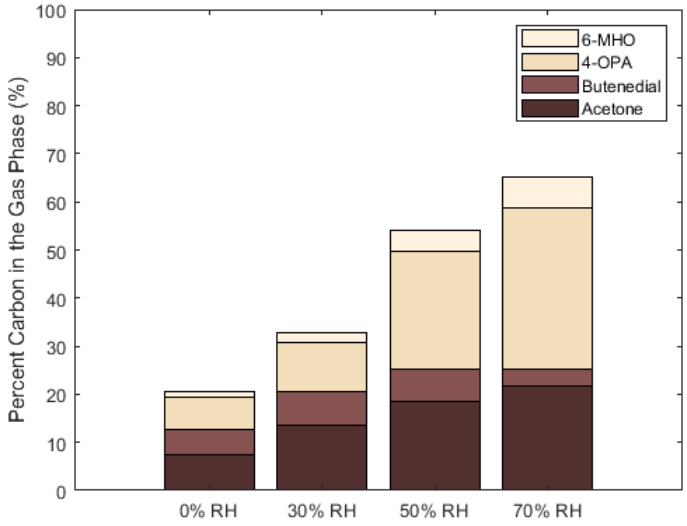

Figure 4: Percent of carbon in the gas phase at 20 ppb h O_3 exposure as a function of RH. Converting the measurements in Figures 2-3 from μg m^{-3} to μg C m^{-3}, and normalizing to the initial concentration of carbon entering the flow tube gives the percent carbon in the gas phase.

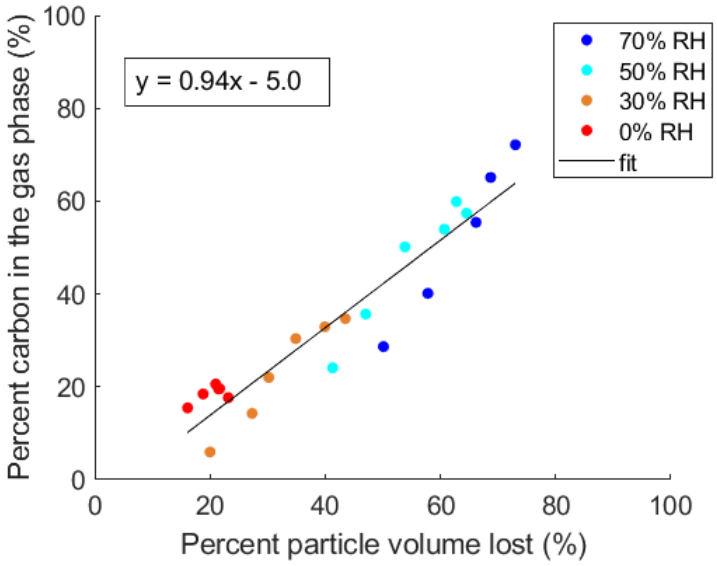

Figure 5: Percent carbon in the gas phase compared to the percent of particle volume lost for all RH and O_3 exposures.

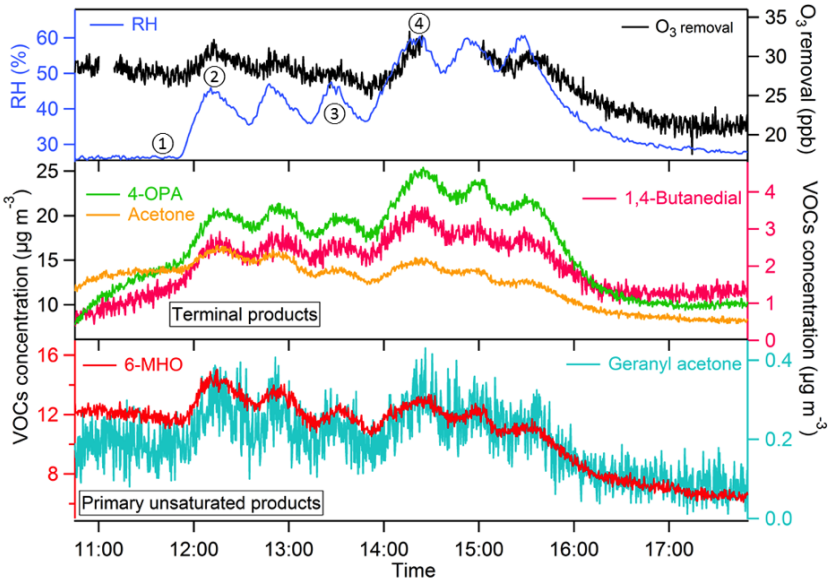

Figure 6: Time series of primary unsaturated products (lower panel) and terminal products (middle panel) with relative humidity and O_3 removal (upper panel) for clothing experiment (O_3 removal was obtained by subtracting measured O_3 level from the level of O_3 in supply air; the gap in the O_3 removal curve is due to the measurement of O_3 level in supply air). Circled numbers in the top panel refer to conditions referenced in Table 1.

Table 1: The concentration change of squalene oxidation products (ΔVOCs, μg m^{-3}) due to relative humidity (RH) increase. Circled numbers refer to points in Figure 6.

RH (%)		ΔO_3 (ppb)	ΔVOCs (μg m^{-3})							
			acetone	4-OPA	6-MHO	geranyl acetone	1,4-butanedial	hydroxy acetone	4-oxobutanoic acid	5-hydroxy-4-oxopentanal
① 26	② 44	2.90	2.17	5.91	2.54	0.117	1.14	1.28	0.340	0.339
③ 46	④ 59	3.37	0.960	5.09	0.652	0.084	0.812	0.881	0.327	0.284

Supporting Information Cover Page

Heterogeneous Ozonolysis of Squalene: Gas-Phase Products Depend on Water Vapor Concentration

Caleb Arata*[†§], Nadja Heine[‡], Nijing Wang[¶], Pawel K. Misztal[§#], Pawel Wargocki[^], Gabriel Bekö[^], Jonathan Williams[¶], William W Nazaroff[‖], Kevin R. Wilson[‡], Allen H. Goldstein[§‖]

[†]Department of Chemistry, [§]Department of Environmental Science, Policy and Management, and [‖]Department of Civil and Environmental Engineering, University of California, Berkeley, California 94720 United States
[‡]Chemical Sciences Division, Lawrence Berkeley National Laboratory, Berkeley, California 94720, United States
[¶]Air Chemistry Department, Max Planck Institute for Chemistry, 55128 Mainz, Germany
[^]Department of Civil Engineering, Technical University of Denmark, 2800 Kgs. Lyngby, Denmark
[#]Now at: Department of Civil, Architectural and Environmental Engineering, The University of Texas at Austin, Austin, TX 78712
*Email: caleb.arata@berkeley.edu

Supporting Information

Pages S1-S8

Tables S1-S5

Figures S1-S4

Table S1: Geranyl acetone concentration data used to calculate production from ozonolysis. Once concentrations were stable in the flow tube reactor, a 'Raw' measurement was taken. Shortly after, the particle flow was replaced with a flow of N_2, and squalene particles were removed from the flow tube reactor, allowing for a background measurement. Background measurements were taken 2 min after the particle flow was removed, when 95% of particles are removed from the flow tube.

RH (%)	O_3 Exposure (ppb h)	Background (μg m^{-3})	Raw (μg m^{-3})	Difference (μg m^{-3})
0	9	9	14	5
0	12	1	4	3
0	17	0	0	0
0	21	0	0	0
0	27	0	0	0
0	32	0	0	0
30	5	69	70	1
30	10	22	37	15
30	12	3	10	7
30	17	0	1	1
30	23	0	0	0
30	30	0	0	0
50	6	149	160	11
50	10	20	34	14
50	12	3	9	6
50	16	0	1	1
50	21	0	0	0
50	26	0	0	0
50	28	0	0	0
70	6	118	127	9
70	9	24	43	19
70	12	3	12	9
70	16	0	1	1
70	21	0	0	0
70	31	0	0	0

Table S2: 6-MHO concentration data used to calculate production from ozonolysis. Once concentrations were stable in the flow tube reactor, a 'Raw' measurement was taken. Shortly after, the particle flow was replaced with a flow of N_2, and squalene particles were removed from the flow tube reactor, allowing for a background measurement. Background measurements were taken 2 min after the particle flow was removed, when 95% of particles are removed from the flow tube.

RH (%)	O_3 Exposure (ppb h)	Background (μg m^{-3})	Raw (μg m^{-3})	Difference (μg m^{-3})
0	9	36	94	57
0	12	15	69	52
0	17	7	31	25
0	21	2	18	15
0	27	1	7	6
0	32	1	3	2
30	5	151	152	1
30	10	112	172	59
30	12	51	132	79
30	17	12	58	45
30	23	6	31	25
30	30	3	13	9
50	6	290	401	115
50	10	105	218	112
50	12	41	169	128
50	16	6	90	83
50	21	2	47	45
50	26	1	27	25
50	28	1	15	14
70	6	240	355	115
70	9	109	260	151
70	12	42	216	173
70	16	6	121	115
70	21	2	68	65
70	31	2	12	11

Table S3: 4-OPA concentration data used to calculate production from ozonolysis. Once concentrations were stable in the flow tube reactor, a 'Raw' measurement was taken. Shortly after, the particle flow was replaced with a flow of N_2, and squalene particles were removed from the flow tube reactor, allowing for a background measurement. Background measurements were taken 2 min after the particle flow was removed, when 95% of particles are removed from the flow tube.

RH (%)	O_3 Exposure (ppb h)	Background (μg m^{-3})	Raw (μg m^{-3})	Difference (μg m^{-3})
0	9	148	185	38
0	12	147	205	58
0	17	134	209	75
0	21	105	202	96
0	27	96	192	95
0	32	101	199	98
30	5	191	229	38
30	10	335	353	19
30	12	378	425	47
30	17	368	492	125
30	23	344	502	160
30	30	337	522	184
50	6	848	887	42
50	10	579	601	20
50	12	712	785	75
50	16	676	917	240
50	21	626	950	323
50	26	618	1020	399
50	28	640	1038	398
70	9	857	871	11
70	12	1083	1165	79
70	16	1233	1516	282
70	21	1179	1630	447
70	31	1136	1734	606

Table S4: 1,4-butanedial concentration data used to calculate production from ozonolysis. Once concentrations were stable in the flow tube reactor, a 'Raw' measurement was taken. Shortly after, the particle flow was replaced with a flow of N_2, and squalene particles were removed from the flow tube reactor, allowing for a background measurement. Background measurements were taken 2 min after the particle flow was removed, when 95% of particles are removed from the flow tube.

RH (%)	O_3 Exposure (ppb h)	Background (μg m^{-3})	Raw (μg m^{-3})	Difference (μg m^{-3})
0	9	81	106	25
0	12	87	126	40
0	17	88	143	55
0	21	67	150	82
0	27	57	142	85
0	32	57	143	85
30	5	66	87	20
30	10	112	135	25
30	12	122	166	45
30	17	110	205	95
30	23	100	218	118
30	30	92	229	135
50	10	153	178	25
50	12	161	207	46
50	16	152	238	86
50	21	146	242	96
50	26	149	257	107
50	28	159	260	101
70	9	189	206	16
70	12	223	246	23
70	16	254	297	43
70	21	239	289	50
70	31	257	309	53

Table S5: Acetone concentration data used to calculate production from ozonolysis. Once concentrations were stable in the flow tube reactor, a 'Raw' measurement was taken. Shortly after, the particle flow was replaced with a flow of N_2, and squalene particles were removed from the flow tube reactor, allowing for a background measurement. Background measurements were taken 2 min after the particle flow was removed, when 95% of particles are removed from the flow tube.

RH (%)	O_3 Exposure (ppb h)	Background (μg m^{-3})	Raw (μg m^{-3})	Difference (μg m^{-3})
0	9	81	167	84
0	12	71	173	102
0	17	71	169	98
0	21	57	165	107
0	27	52	154	102
0	32	52	158	105
30	5	105	137	32
30	10	142	227	84
30	12	123	267	141
30	17	92	293	197
30	23	81	289	206
30	30	75	288	213
50	6	163	240	77
50	10	135	249	112
50	12	110	289	178
50	16	71	301	230
50	21	62	302	238
50	26	60	319	256
50	28	62	307	243
70	6	137	216	77
70	9	158	293	133
70	12	142	337	194
70	16	122	381	258
70	21	149	428	278
70	31	184	459	278

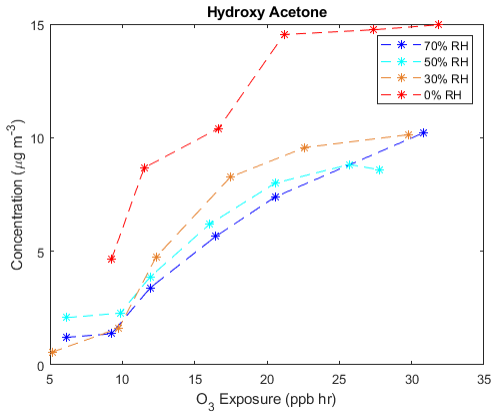

Figure S1: Hydroxy acetone concentration as a function of humidity and O_3 exposure.

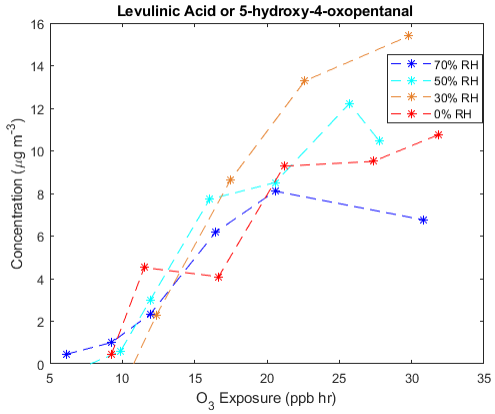

Figure S2:5-hydroxy-4-oxopentanal and levulinic acid concentration as a function of humidity and O_3 exposure.

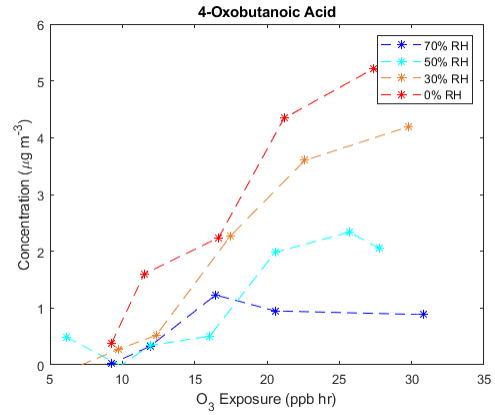

Figure S3: 4-oxopentanoic acid concentration as a function of humidity and O_3 exposure.

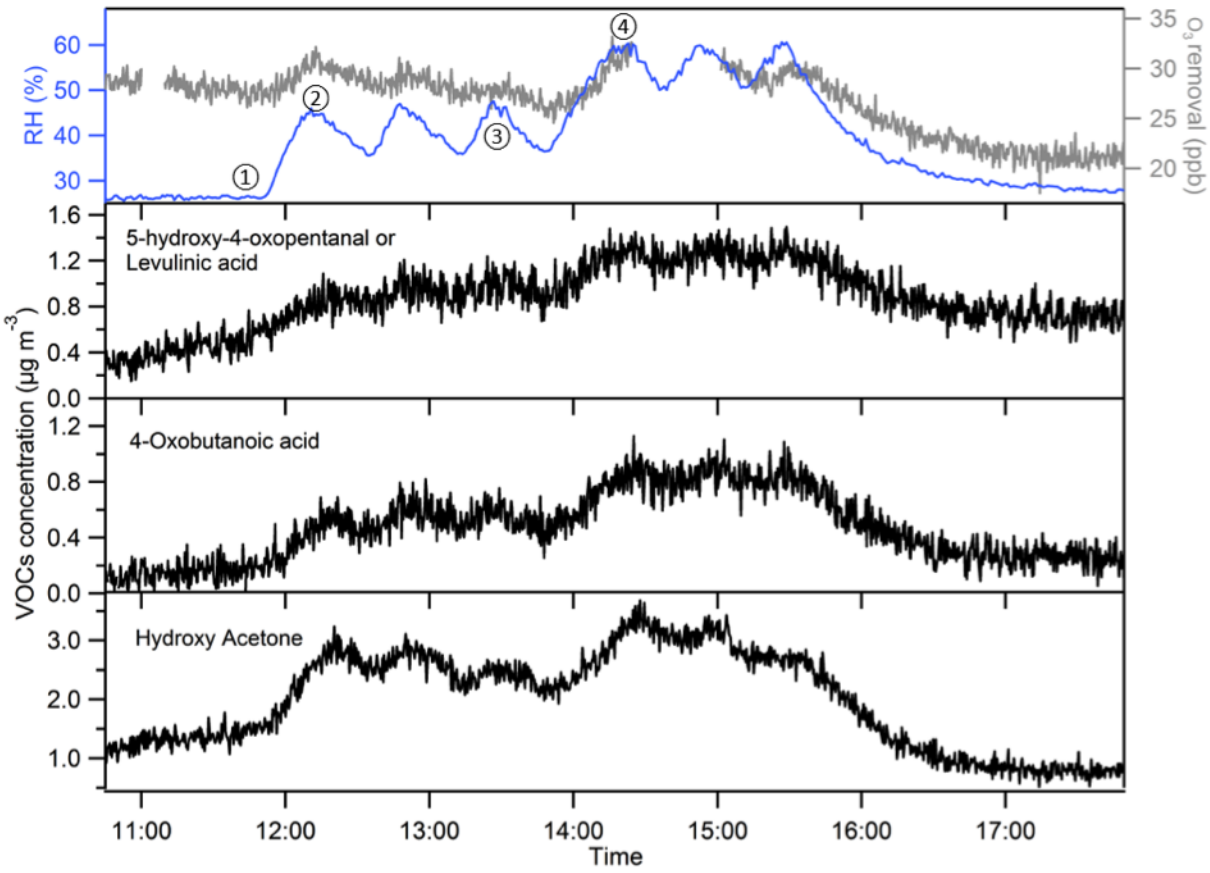

Figure S4: Time series of other squalene oxidation products with relative humidity and O_3 removal (upper panel) for the clothing experiment (O_3 removal is the difference between O_3 measured in supply air and the chamber; the data gap is due to the supply air measurement).